RSC Advances

RSC Advances

www.rsc.org/advances

ROYAL SOCIETY OF CHEMISTRY

www.rsc.org/advances

Theoretical Study on the Radical Reaction Mechanism in the Cross-linking Process of Polyethylene

HUI ZHANG[1,*], YAN SHANG[1], MINGXIA LI[2,†], HONG ZHAO[1], XUAN WANG[1], BAOZHONG HAN[1,‡]

[1]*Key Laboratory of Engineering Dielectrics and Its Application of Ministry of Education & College of Chemical and Environmental Engineering, Harbin University of Science and Technology, Harbin 150080, People's Republic of China*
[2]*Key Laboratory of Functional Inorganic Material Chemistry of Education Ministry and Laboratory of Physical Chemistry, School of Chemistry and Materials Science, Heilongjiang University, Harbin 150080, People's Republic of China*

Abstract: Theoretical investigation on the radical-initiated reactions of the polyethylene cross-linking process with the voltage stabilizer grafting is accomplished by density functional theory (DFT) calculations. At B3LYP/6-311+G(d,p) level, the molecular properties of 22 reactions and reaction potential energy information of 18 radical-initiated reactions are obtained. The HOMO-LUMO energy gaps, ionization potentials, and electron affinities of the cross-linking agent, voltage stabilizer, antioxidant, and by-product in the polyethylene insulation composite are calculated. The results show that the by-product, cross-linking agent, and voltage stabilizer can effectively increase the electrical breakdown strength. In addition, aromatic ketone voltage stabilizer and hindered phenol antioxidants of the studied molecule can be grafted to polyethylene chain easily during the polyethylene cross-linking process, and they have excellent compatibility with polymers matrix. The investigation is expected to provide reliable information for optimizing process and for the development of the insulation material of high-voltage cable exceed 500 kV in real applications.

Key words: polyethylene; transition states; radical; cross-link process

---

*Corresponding author Fax: +86-451-86392708; e-mail: hust_zhanghui11@hotmail.com
†Corresponding author Fax: +86-451-86604331; e-mail: limingxiaxxq@sina.com
‡Corresponding author Fax: +86-451-86391659; e-mail: hbzhlj@163.com

1. Introduction

Cross-linked polyethylene (XLPE) with excellent dielectric property and chemical corrosion resistance has become one of most widely applied insulation materials for high voltage cables up to 500 kV in real application. The mechanical properties and the capable of heat resistance of polyethylene (PE) are raised significantly through cross-linking process. Therefore, the chemical reactions during cross-linking of PE play a crucial role in designing and developing insulation materials for high voltage cables. The pre-breakdown degradation phenomenon known as electrical treeing initiates at points of high and divergent electric field is associated with partial discharges and insulation failure in the power cable [1,2]. Therefore the rated voltage of XLPE insulated power cable is limited to 500 kV even though the XLPE compound was manufactured with super-clean technology removing the impurities more than 50 μm to quarantine uniformity of insulating wall of the cable. Some organic additives, such as polycyclic aromatic compounds or those with benzophenone-like structures, can serve as so-called voltage stabilizers to effectively increase the resistance to electrical treeing [3-8]. This may be the next solution for the XLPE insulating compound for the power cable insulation exceed 500 kV. Recently, our research group employed both experimental and computational method to study the effect of acetophenone as voltage stabilizers. The addition of acetophenone, a prototypical aromatic ketone compound, leads to a 50% increase of the alternate current (AC) electrical breakdown strength of XLPE [9]. By the theoretical studies, we foremost elucidated that keto-enol tautomerism of aromatic carbonyl compounds is one of the important factors for inhibiting initiation and propagation of electrical treeing in polyethylene, and proposed the mechanisms of aromatic carbonyl compounds as voltage stabilizers for increasing the electrical breakdown strength of

XLPE in 2013 [10-12]. However, the compatibility of acetophenone with XLPE matrix is poor, which is easy to migrate out of polymeric matrix, leading to worse performance of PE insulation materials. In 2012, a benzil-type compound with a larger alkoxy chain was evaluated as voltage stabilizer in a super-clean XLPE by Jarvid and his co-workers [7]. As a result, the electrical treeing inception level was effectively raised, and the compatibility with PE matrix was also significantly improved. After that, the synthesis and physico-chemical properties of seven benzil-type voltage stabilizers were also reported by Jarvid and his co-workers [8]. These additives substantially enhance the dielectric strength of the insulating material under high-voltage alternating current conditions. The dielectric strength, 70% higher than the reference XLPE, was improved by the addition of the voltage stabilizers with short (methyl) side chains linked to the benzil core via an ester or tertiary amine group [8]. This inspired us that the excellent compatibility of voltage stabilizer with PE matrix can improve the electrical breakdown strength of XLPE, namely, if PE molecule chain can react with voltage stabilizer molecule grafting to yield stationary products during the cross-linking process, XLPE insulation materials can possess of permanent insulation performances age long.

Is the grafting of the voltage stabilizer molecule to the PE molecule chain possible in the cross linking process?

Firstly we review the production processes and chemical reactions in the processes. The production process of cross-linkable PE insulation material for high voltage cable: (1) LDPE and antioxidant with a certain ratio were mixed and fed into the screw mixer at 115 °C-180 °C. The super-clean granular LDPE/antioxidant blend was produced through subsequent filtration, extrusion, pelletizing, and drying. (2) The LDPE/antioxidant blend was put in the tumbler mixer. The mixer was rolled and the

cylinder wall was heated to 80 °C. Certain amount of liquid DCP at 80 °C was injected into the mixer according to the ratio. After 40 min, the mixer was stopped and DCP had soaked into the granular material. (3) The granular material with DCP was put in the constant temperature storage tank under 80 °C for 15 to 20 hours to keep DCP uniform in the granules. And then, the material was transferred to the finished product tank to get cross-linkable PE insulation material.

The extrusion and cross linking process of cross-linkable PE insulation material for high voltage cable: (1) The cross-linkable PE insulation material was extruded outside the cable conductor under 115 °C-120 °C; (2) The cable insulation produced cross linking reaction at vulcanization tube full of nitrogen under a pressure of 0.6-1MPa and an insulation temperature of 280 °C. Then the material was cooled to room temperature in nitrogen.

During the cross-linking process of a high-temperature tube, a lot of complicated reactions occur. For example, decomposition reactions (DCp $\rightarrow$ 2·Cp and ·Cp $\rightarrow$ Ap + ·CH$_3$), isomerization reactions (Ap $\rightarrow$ PAp and Vp $\rightarrow$ PVp), and radical reactions (·CH$_3$ with Pe8, Vp, and Bp; ·Cp with Pe8, Vp, and Bp). The chemical reaction equations of the possible radical-initiated reactions in the upper production processes summarize in Table 1.

Then we try to investigate the reaction process of PE cross linking with the present of voltage stabilizer using density functional theory (DFT) [13] calculations in this paper to study the possibilities of voltage stabilizer grafting. Main materials for preparing XLPE generally include low density polyethylene (LDPE), antioxidant (to be used to improve the thermo and oxygen aging property of PE), voltage stabilizer, and peroxide cross-linker (such as dicumyl peroxide, DCP). In this work, three molecules, 4-methylheptane (Pe8), valerophenone (Vp), and

2,6-Di-*t*-butyl-4-*n*-butylphenol   (Bp),   are   selected   as   model   molecules   of cross-linkable PE, voltage stabilizer, and hindered phenol antioxidant, respectively. The molecular formula, molecular name, and corresponding abbreviations of the possibly molecules during the cross-linking process are listed in Table 2. Cumyl peroxide (CP) radical is originated from the homolytic bond cleavage of cross-linking agent DCP, and by-products are formed after the following decomposition reaction of CP radical, such as 2-phenyl-isopropoxy radical, CH_3 radical, acetophenone *etc* [14]. CP and CH_3 radicals can undergo hydrogen abstraction reaction with PE molecule chain, voltage stabilizer molecule chain, and antioxidant molecule chain to form the corresponding radicals. These corresponding free radicals will react with each other to produce inactive products. Polyethylene (PE) molecule chain radicals can not only react with other PE molecule chain radicals to form cross-linking polyethylene, but also work with molecule radicals of voltage stabilizer and antioxidant to yield stationary products, which leads to the grafting of voltage stabilizer and antioxidant to the PE chain and the improving compatibility between polymers matrix and additives.

To the best of our knowledge, no theoretical work has addressed on the radical-initiated reactions of the polyethylene cross-linking process with the present of voltage stabilizer at atomic and molecular levels. There is a potential demand for the theoretical understanding of voltage stabilizer grafting to the PE molecule chain during cross-linking process at atomic and molecular levels. In this paper, we aim at providing a systematic investigation on the possibility of the radical reaction and the dominant reaction channel during the polyethylene cross-linking process with the present of voltage stabilizer. The cross-linking radical reaction mechanism would be proposed on the basis of the theoretical study, which would be useful for the rational molecular design and synthesis of the desired voltage stabilizers for real applications.

2. Computational Methods

DFT [13] has been selected to optimize the geometries of the studied molecules. Comparisons between the computational values of the adiabatic ionization potentials IP(a) and the electron affinities EA(a) from various theoretical methods [15-24] and the corresponding experimental vales [25] are listed in Table 3. The frequencies of the stationary points have one or two imaginary frequency resulting in that IP(a) values cannot be obtained and have to be labeled by "--" in Table 3. The HF/6-31G* method generates larger deviations from experiment comparing to the theoretical (B3LYP, PBE, and MP2) method. Among the tested functional and basis set levels, B3LYP/6-311+G(d,p) calculations show best agreement with the experiment values especially for EA(a) of Ap. The theoretical values are in good agreement with the corresponding available experimental values [25], which indicates that the theoretical results in this paper are reasonable and reliable. In this paper, the equilibrium geometries of all the stationary points of the neutral and ion states of the studied molecules are optimized at the ground state S_0 using B3LYP [16-19] functional with the 6-311+G(d,p) basis set, and the frequencies are also obtained at the same method. On the basis of these calculations, the energy gap (E_g) between the highest occupied molecular orbital (HOMO) and the lowest unoccupied molecular orbital (LUMO), the ionization potential (IPs), and the electron affinity (EAs) are obtained. The equilibrium geometries and frequencies of reactants, transition states, and products of the studied reactions at the ground state S_0 are obtained at the same level. The minimum energy path (MEP) is obtained by intrinsic reaction coordinate (IRC) theory with a gradient step-size of 0.05 (amu)$^{1/2}$ bohr. Then, the first and second energy derivatives are obtained to calculate the curvature of the reaction path and the generalized vibrational frequencies along the reaction path. All the electronic structure

calculations are performed using GAUSSIAN09 program package [26]. The relevant

schematic formulae can be defined as follows,

$IP(v) = E^+(M) - E(M)$

$IP(a) = E^+(M^+) - E(M)$

$EA(v) = E(M) - E^-(M)$

$EA(a) = E(M) - E^-(M^-)$

where $E^+(M^+)$, $E^-(M^-)$, and $E(M)$ represent the energies of the cation, anion and

neutral species in their lowest energy geometries, respectively; while $E^+(M)$ and $E(M^+)$

refer to the energies of cation and neutral species with the geometries of neutral and

cation, respectively; $E^-(M)$ and $E(M^-)$ are the energies of anion and neutral species

with the geometries of neutral and anion, respectively; where v and a represent

vertical energy based on the geometry of the neutral molecule and adiabatic energy

from the optimized structure for both the neutral and charged molecule, respectively.

Schematic description of geometric coordinate modifications and energy changes are

illustrated in Figure 1.

3. Results and Discussion

3.1. Stationary point geometries

The optimized geometric structures on S_0 state of the studied molecules at the

B3LYP/6-311+G(d,p) level, involving the reactants, transition states, and products of

2 isomerization reactions, 2 decomposition reactions, and 18 radical reactions are

presented in Figure 2. Optimized bond lengths of breaking and forming bonds for the

21 transition states, the corresponding reactant C—C or C—H bonds, and the product

O—H or C—H bond, and calculated harmonic vibrational frequencies in its S_0 states

at the B3LYP/6-311+G(d,p) level are listed in Table 1. All the transition states are

confirmed by normal-mode analysis to have only one imaginary frequency

corresponding to the stretching modes of the coupling breaking and forming bonds. The others harmonic vibrational frequencies are confirmed by normal-mode analysis to have real frequency corresponding to all of the vibrating modes. The transition states are abbreviated to the corresponding TS, reaction pathways are represented to R. In Table 1, it can be seen that for the transition state structure on S_0 states of the two studied isomerization reactions, the elongation of the C—H breaking bond in keto-tautomer is larger than that of the product-forming O—H bond in equilibrium enol-tautomer, indicating that two isomerization reactions are product-like, i.e., the reactions will proceed *via* "late" transition states for an endothermic reaction., which is consistent with Hammond's postulate [27]. It also can be seen that the other transition state structures of the studied radical reactions on its S_0 state have a common character, the elongation of the breaking bond is smaller than that of the forming bond, they are all reactant-like, i.e., those reaction pathways will proceed *via* "early" transition states for an exothermic reaction [27].

3.2. Energies: Frontier MOs, IPs, and EAs

Both the ionization potentials (IPs) and the electron affinities (EAs) of the molecules are the important parameters to characterize the reduction and oxidation ability, respectively. As shown in Table 4, the calculated values of the vertical and adiabatic IPs, EAs at the B3LYP/6-311+G(d,p) level and the corresponding experimental data [25] (in bracket) are listed, as well as the calculated HOMO-LUMO energy gap (E_g). The varied trends of the ionization potentials and electron affinities are similar to those of the negative value of the HOMO and LUMO energies, respectively. The ability of accepting hot electron is closely related to LUMO. The relative orderings of LUMO energies provide a reasonable qualitative description of the ability to accept electron. In Table 4, there are σ electrons in 4Pe,

6P, and 8Pe, the value of E_g depends on the energy difference between orbital σ and σ* (σ → σ*). Thus, E_g decreases with the increasing carbon chain, the value of E_g (Vp) is also lower than that of Ap. Carbonyl, phenyl, and heteroatom groups are efficacious to decrease E_g. Comparing with aliphatic chain, the introduction of carbonyl group and phenyl group into the molecule are propitious to electronic dissociation because of the high HOMO energy levels and small ionization potentials in terms of Koopmans' theorem, in addition, it is also favorable for electron to be accepted if the molecule possesses low LUMO energy levels and large electron affinities energies. The value of E_g is defined as the energy gap between orbital π and π* (π → π*) when introducing phenyl into the molecule, which is smaller than that of σ → σ*, thus, E_g (DCP) < E_g (4Pe, 6Pe, and 8Pe). Besides, the alkyl groups linked to benzene ring in DCP will exhibit σ-π super-conjugated effect. The carbonyl group linked to benzene ring in Ap will exhibit π-π conjugated effect. The degree of π-π conjugated is stronger than that of σ-π, thus, E_g (Ap) < E_g (DCP). Comparing with Ap, as two benzene rings are linked with a carbonyl group directly in Bz, the π-π-π conjugated effect is present, the conjugated system expands, the value of E_g decreases. Similarly, as the two benzene rings link with difference carbonyls in Ben, a larger π-π-π-π conjugated effect is formed, such as, E_g (Ben, 4.23 eV) < E_g (Bz, 4.90 eV) < E_g (Ap, 5.20 eV). Comparing with Bz and Ben, not only π-π-π and π-π-π-π conjugated effects between carbonyl groups and benzene rings are formed in Bzo and Bd, respectively, but also p-π conjugated effect is also formed, as -OR groups are linked to benzene ring, the conjugated systems are larger, as the result, it can be concluded that E_g (Bd) < E_g (Ben), E_g (Bzo) < E_g (Bz). The calculated results have been well explained by Jarvid, Englund, and their co-worker [6-8], they concluded that the introduction of carbonyl and alkoxy into benzophenone molecules is an exciting

molecular design because they can effectively decrease E_g value and possess excellent compatibility with polymers matrix. Such E_g of Bzo (4.44 eV) and Bd (4.22 eV) are smaller than that of Bz and Ben, respectively. The energy of electronic transition is smaller when E_g decreases. In addition, the -OR group in Bzo and Bd will exhibit inductive electron-donating effects, which makes the electron densities of benzene ring in Bzo and Bd are larger than those of Ben and Bz. The electron density on benzene ring is larger, the ability to accept electron is weaker. For instance, EA(a) (Bzo, 0.40 eV) < EA(a) (Bz, 0.73 eV) and EA(a) (Bd, 1.28 eV) < EA(a) (Ben, 1.53 eV). There are two carbonyl groups in Ben, and one carbonyl group in Bz. The electron density on benzene ring in Bz is larger than that of Ben, then EA (Bz) < EA (Ben). Comparing with alkyl, carbonyl is electron-withdrawing group, -OR is electron-donating group, the electron density on benzene ring in Bp is larger than that of Vp, resulting in the ability to accept electron is weaker in Bp than that of Vp, and EA (Bp, -0.73) < EA (Ben, 0.33).

According to the production process of cross-linkable polyethylene insulation material for high voltage cable, the by-product, superfluous cross-linking agent, voltage stabilizer, and antioxidant are usually adulterated in the polyethylene insulation composite product, such as, the studied model molecules DCP, Ap, Vp, and Bp. These molecules with carbonyl or benzene ring possess larger EA(a) than 8Pe and smaller IP(v) values than 8Pe due to their low LUMO and high HOMO energy levels. They possess lower barriers to accept electrons because of their lower LUMO energy levels than that of aliphatic chain. For example, DCP possesses lower LUMO level than Bzo and hence exhibits better electron trapping ability. Thus, these conjugated aromatic carbonyl or benzene ring molecules possess stronger capability of trapping electron than that of aliphatic chain. They are also possess lower IP(v) than 8Pe, and

give rise to collision ionization before polyethylene chain has been ionized, it can prevent the degradation of the polymer matrix when these conjugated aromatic carbonyl or benzene ring molecules are doped into polyethylene compound, which is consistent with Ashcraft's suggestion [1].

The carrier (electron) may appear in XLPE insulated high-voltage cable. The initial electron may be created by electrode emission under the local high electric field, the initial electron which gains enough kinetic energy under the electric field in insulation material is known as hot electron, it can cause dielectric breakdown. The superfluous cross-linking agent and aromatic ketone molecules in XLPE insulation composite product can trap the hot electron and decrease the kinetic energy of the hot electron, so as to the "hot electron" have not enough energy to break the C-C bonds of XLPE. In addition, DCP, Bp, and aromatic ketone molecules can decrease E_g by decreasing transition energy, which should be less than C-C bond cleavage energy. Thus, they can accomplish the electronic transition to dissipate hot electron energy, and prevent degradation of the polymer matrix. In this way, it can effectively inhibit the initiation and propagation of XLPE electrical treeing and simultaneously strengthen the electrical breakdown strength that XLPE can endure. As a consequence, the insulating XLPE material exhibits an elevated AC breakdown strength. The detailed mechanism about increasing the breakdown strength of XLPE may provide reliable information for future experimental investigations.

3.3. Energetics

The reaction enthalpies at 298 K (ΔH_{298}^0) and the potential barrier heights (ΔE^{TS}) with zero-point energy (ZPE) corrections for the studied reactions on S_0 state obtained base on the electronic structure calculations at the B3LYP/6-311+G(d,p) level are listed in Table 5, as well as the relative breaking bond dissociation energies (D_{298}^o).

Breaking bond dissociation energies are closely related to the corresponding reaction potential barrier heights. Bond dissociation energy of H atom in hydroxyl of antioxidant is lower than that of H-Bp4 (or Bp3, Bp2), for instance, bond dissociation energy of H atom in hydroxyl of antioxidant Bp is 3.12 eV, and H atom in alkyl of H-Bp2 is 4.05 eV. It means that antioxidants are often used to kill free radicals in XLPE insulation materials for high voltage cables. To test the stability of the TSs, the basis set superposition error (BSSE) correction is estimated using the counterpoise method. The energies of BSSE at the B3LYP/6-311+G(d,p) level are also listed in Table 5. It can be found that the BSSE energies are small. Here, we aim at understanding the possibility of the radical reaction formation of Vp and Bp to compare with Pe8 during the polyethylene cross-linking process. Thus, single-point energy correction has not been done. Experimental data of acetophenone in the lowest five electronically excited states (T_1, S_1, T_2, S_2, and S_3) and the calculated values were reported from our previous work [11]. The calculated ΔE^{T1-S0} (the relative energy margins between S_0 and T_1 states) at QCISD(T)//B3LYP level of acetophenone is 74.92 kcal/mol, showing good consistency with the reported value of 73.74 kcal/mol [28]. Experimental value of ΔE^{S0-S1} (the relative energy margins between S_0 and S_1 states) is 77.99 kcal/mol [28]. The calculated ΔE^{S0TS} of acetophenone at B3LYP/6-311+G(d,p) level is 62.31 kcal/mol (2.70 eV). The mechanisms of aromatic carbonyl compounds as voltage stabilizers for increasing the breakdown strength of XLPE have been firstly proposed on the basis of our theoretical results [11-12]. In addition, keto-enol and valence bond isomerization is suggested to occur when acetophenone is used as voltage stabilizer [10]. From Table 5, it can be seen that the D^o_{298} of the breaking bond in CP radical is negative (-0.27 eV), meaning that the product CH$_3$ radical of CP radical dissociation reaction is high active than CP radical,

CH$_3$ radical is transient state. The dissociation reaction of DCP is barrierless reaction, and the D_{298}^{o} of the breaking bond in DCP is smaller than those of Pe8, Vp, and Bp, showing that the dissociation reaction of DCP is more easier during the polyethylene cross-linking process, resulting in the formation of CP and CH$_3$ radicals. Then radical-initiated reaction with Pe8, Vp, and Bp are following occurred. The potential barriers of ·CP radical-initiated reaction are smaller than that of the corresponding reaction of ·CH$_3$ radical-initiated, except for the reaction for the formation of VP3. For the studied radical-initiated reaction, the formation reaction of Vp is easier than that of the corresponding Pe8 radicals. For instance, the potential barriers of formation of RVp4 are smaller than that of the corresponding formation reaction of RPe84. Because of the H atom of breaking bond in Vp is more active than that in Pe8 due to the larger electronegativity of O than that of C. Therefore, the H in Vp can dissociate easily and lead to more facile Vp4 radical with the lower energy barriers. In addition, aromatic ketone exhibits conjugated effect at the same time in Vp4. It further impels the transfer of π electrons to O atom in –C=O, which in turn exerts stronger attraction to H atom in acetyl, and thus isomerization occurs in an easier fashion. Thus, Vp can linked to the chain of PE during the polyethylene cross-linking process. The similar case is also found in radical-initiated reactions of Bp. The radical-initiated reactions listed Table 5 are exothermic reactions. The two keto-enol isomerization reactions possess energy barriers, and both are endothermic reactions. The calculated results show that the reaction potential barrier heights of keto-enol isomerization reactions (RAp and RVp) decrease with the increase of carbon chain number, since alkyl group exhibit inductive electron-donating effect and σ-π super-conjugated effect. As a result, less amount of energy about 62.31 kcal/mol (2.70 eV) is needed to complete the keto-enol isomerization, which is much lower than that for the carbon-carbon single

bond energy (the average bond energy is 82.95 kcal/mol) in XLPE. The above results indicate that the studied aromatic ketone molecules can undergo isomerization reaction, absorbing and transferring the energy of hot electrons when hot electrons are injected into polyethylene compound. The studied aromatic ketone molecules Vp may be effective as voltage stabilizer in real application for increasing the breakdown strength of insulating XLPE material as it can bond to PE chain during the cross-linking process in a high-temperature tube. Further work to account for structural and electronic properties of nanocomposites enlaced by PE (like as single-walled carbon nanotubes [29]) is under way.

4. Conclusion

A systematically theoretical study on the radical reaction mechanisms in the polyethylene cross-linking process has been carried out at the atomic and molecular levels. Aromatic ketone voltage stabilizer Vp and hindered phenol antioxidants Bp molecules can be linked to PE chain during the polyethylene cross-linking process. The superfluous cross-linking agent, by-product, and adulterant molecules in XLPE insulation composite product with carbonyl, phenyl, alkoxy, and heteroatom groups can effectively prevent the hot electrons bombarding C-C bond of XLPE matrix. The suggested mechanism for increasing the breakdown strength of XLPE may provide reliable information to optimize the cross-linking process, to select the antioxidants, and to design the perfect voltage stabilizer for real applications.

Acknowledgements

Reference

[1] Ashcraft AC, Eichhorn RM, Shaw RG (1976) Laboratory Studies of Treeing in Solid Dielectrics and Voltage Stabilization of Polyethylene, IEEE Intern Sympos Electr Insul, pp. 6

[2] Jarvid M, Johansson A, Englund V, Lundin A, Gubanski S, Müller C, Andersson MR (2015) High Electron Affinity: A Guiding Criterion for Voltage Stabilizer Design, J Mater Chem A, 3: 7273-7286

[3] Yamano Y, Endoh H (1998) Increase in Breakdown Strength of PE Film by Additives of Azocompounds, IEEE Transactions on Dielectrics and Electrical Insulation, 5: 270-275

[4] Yamano Y (2006) Roles of Polycyclic Compounds in Increasing Breakdown Strength of LDPE Film, IEEE Transactions on Dielectrics and Electrical Insulation, 13: 773-781

[5] Yamano Y, Iizuka M (2009) IEEE Transactions on Dielectrics and Electrical Insulation 16(1): 189-198

[6] Englund V, Huuva R, Gubanski SM (2009) IEEE Transactions on Dielectrics and Electrical Insulation 16(5): 1455-1460

[7] Jarvid M, Johansson A, Englund V, Gubanski S, Andersson MR (October 2012) Electrical Tree Inhibition by Voltage Stabilizers, Annual Repot Conference on Electrical Insulation and Dielectric Phenomena, pp. 605-608

[8] Jarvid M, Johansson A, Bjuggren JM, Wutzel H, Englund V, Gubanski S, Müller C, Andersson MR (2014) Tailored Side-Chain Architecture of Benzil Voltage Stabilizers for Enhanced Dielectric Strength of Cross-Linked Polyethylene, J Poly Sci, Part B: Polymer Physics, 52(16): 1047-1054

[9] Zhang H, Shang Y, Zhao H, Han BZ, Li ZS (2015) Study of the Effect of

RSC Advances Accepted Manuscript

Valence Bond Isomerizations on Electrical Breakdown by Adding Acetophenone to Polyethylene as Voltage Stabilizers, Comput Theor Chem, 1062: 99-104

[10] Zhang H, Shang Y, Zhao H, Han BZ, Li ZS (2013) Mechanisms on Inhibition of Polyethylene Electrical Tree Aging: A Theoretical Study, J Mol Model 19: 3035-3044

[11] Zhang H, Shang Y, Zhao H, Han BZ, Li ZS (2013) Mechanisms on Electrical Breakdown Strength Increment of Polyethylene by Acetophenone and its Analogues Addition: A Theoretical Study, J Mol Model, 19: 4477-4485

[12] Zhang H, Shang Y, Wang X, Zhao H, Han BZ, Li ZS (2013) Mechanisms on Electrical Breakdown Strength Increment of Polyethylene by Aromatic Carbonyl Compounds Addition: A Theoretical Study, J Mol Model 19: 5429-5438

[13] Parr RG, Yang W (1989) Density-functional Theory of Atoms and Molecules, Oxford University Press: New York

[14] Markert H, Wiedenmann R (1973) Crosslinking of polyethylene in the presence of additives Part 1, Siemens Forsch. Und Entwickl. Ber. 2(2): 85-91

[15] McWeeny R, Dierksen G (1968) Self-consistent Perturbation Theory. 2. Extension to Open Shells, J Chem Phys, 49: 4852

[16] Truong TN, Duncan WT, Bell RL (1996) Chemical Applications of Density-Functional Theory. American Chemical Society, Washington, DC, p85

[17] Lee C, Yang W, Parr RG (1988) Development of the Colle-Salvetti Conelation Energy Formula into a Functional of the Electron Density, Phys Rev B 37: 785-789

[18] Miehlich B, Savin A, Stoll H, Preuss H (1989) Results Obtained with the Correlation Energy Density Functionals of Becke and Lee, Yang and Parr, Chem

Phys Lett 157: 200-206

[19] Becke AD (1993) Density-functional Thermochemistry. III. The Role of Exact Exchange, J Chem Phys 98: 5648-5652

[20] Perdew JP, Burke K, Ernzerhof M (1996) Generalized Gradient Approximation Made Simple, Phys Rev Lett, 77: 3865-3868

[21] Perdew JP, Burke K, Ernzerhof M (1997) Errata: Generalized Gradient Approximation Made Simple, Phys Rev Lett, 78: 1396

[22] Duncan WT, Truong TN (1995) J Chem Phys, 103: 9642-9652

[23] Frisch MJ, Head-Gordon M, Pople JA (1990) Direct MP2 Gradient Method, Chem Phys Lett, 166: 275-280

[24] Head-Gordon M, Pople JA, Frisch MJ (1988) MP2 Energy Evaluation by Direct Methods, Chem Phys Lett, 153: 503-506

[25] Lias SG, Bartmess JE (2011) In NIST ChemistryWebBook, NIST Standard Reference Database Number 69

[26] Frisch MJ, Trucks GW, Schlegel HB, Scuseria GE, Robb MA, Cheeseman JR, Scalmani G, Barone V, Mennucci B, Petersson GA, Nakatsuji H, Caricato M, Li X, Hratchian HP, Izmaylov AF, Bloino J, Zheng G, Sonnenberg JL, Hada M, Ehara M, Toyota K, Fukuda R, Hasegawa J, Ishida M, Nakajima T, Honda Y, Kitao O, Nakai H, Vreven T, Montgomery JA, Jr, Peralta JE, Ogliaro F, Bearpark M, Heyd JJ, Brothers E, Kudin KN, Staroverov VN, Kobayashi R, Normand J, Raghavachari K, Rendell A, Burant JC, Iyengar SS, Tomasi J, Cossi M, Rega N, Millam JM, Klene M, Knox JE, Cross JB, Bakken V, Adamo C, Jaramillo J, Gomperts R, Stratmann RE, Yazyev O, Austin AJ, Cammi R, Pomelli C, Ochterski JW, Martin RL, Morokuma K, Zakrzewski VG, Voth GA, Salvador P, Dannenberg JJ, Dapprich S, Daniels AD, Farkas O, Foresman JB,

Ortiz JV, Cioslowski J, Fox DJ (2009) Gaussian, Inc., Revision A.02, Wallingford CT

[27] Hammond GS (1955) A Correlation of Reaction Rates, J Am Chem Soc 77: 334-338

[28] Ohmori N, Suzuki T, Ito M (1988) Why does intersystem crossing occur in isolated molecules of benzaldehyde, acetophenone, and benzophenone? J Phys Chem 92:1086-1093

[29] Suggs K, Wang XQ (2010) Structural and Electronic Properties of Carbon Nanotube-reinforced Epoxy Resins, Nanoscale, 2: 385-388

Table 1. Optimized bond lengths of breaking/forming bonds (b/f) for the studied transition states, and the corresponding reactant bonds, product bonds (all in angstrom), and calculated breaking/forming bond frequencies (in cm^{-1}) on ground state S_0 at the B3LYP/6-311+G(d,p) level.

reaction equation	reactant	b/f	product	freq.
(Ph)C(CH$_3$)$_2$–O–O–C(CH$_3$)$_2$(Ph) → 2 (Ph)C(CH$_3$)$_2$–O•	1.471	--/--	--	--
(Ph)C(CH$_3$)$_2$–O• → (Ph)C(CH$_3$)=O + •CH$_3$	1.537	2.095/--	--	464 i
(Ph)C(CH$_3$)=O → (Ph)C(CH$_2$)–OH	1.089	1.491/1.275	0.963	2175 i
enolization structure	1.092	1.493/1.284	0.964	2195 i
branched alkane + •CH$_3$ → radical + CH$_4$	1.100	1.296/1.437	1.091	1511 i
branched alkane + •CH$_3$ → radical + CH$_4$	1.098	1.311/1.414	1.091	1590 i
branched alkane + •CH$_3$ → radical + CH$_4$	1.097	1.307/1.410	1.091	1572 i
alkane + (Ph)C(CH$_3$)$_2$–O• → radical + (Ph)C(CH$_3$)$_2$–OH	1.100	1.265/1.317	0.962	1410 i
alkane + (Ph)C(CH$_3$)$_2$–O• → radical + (Ph)C(CH$_3$)$_2$–OH	1.098	1.278/1.286	0.962	1546 i
alkane + (Ph)C(CH$_3$)$_2$–O• → radical + (Ph)C(CH$_3$)$_2$–OH	1.097	1.244/1.320	0.962	1253 i
ketone + •CH$_3$ → radical + CH$_4$	1.098	1.268/1.472	1.091	1370 i
ketone + •CH$_3$ → radical + CH$_4$	1.095	1.311/1.402	1.091	1587 i
ketone + •CH$_3$ → radical + CH$_4$	1.097	1.308/1.410	1.091	1572 i
ketone + (Ph)C(CH$_3$)$_2$–O• → radical + (Ph)C(CH$_3$)$_2$–OH	1.098	1.269/1.296	0.962	1569 i
ketone + (Ph)C(CH$_3$)$_2$–O• → radical + (Ph)C(CH$_3$)$_2$–OH	1.095	1.262/1.304	0.962	1495 i
ketone + (Ph)C(CH$_3$)$_2$–O• → radical + (Ph)C(CH$_3$)$_2$–OH	1.097	1.245/1.319	0.962	1258 i

1.096	1.261/1.493	1.091	1363 *i*
1.097	1.308/1.405	1.091	1581 *i*
1.098	1.302/1.412	1.091	1556 *i*
1.096	1.225/1.400	0.962	922 *i*
1.097	1.245/1.317	0.962	1266 *i*
1.098	1.248/1.321	0.962	1341 *i*
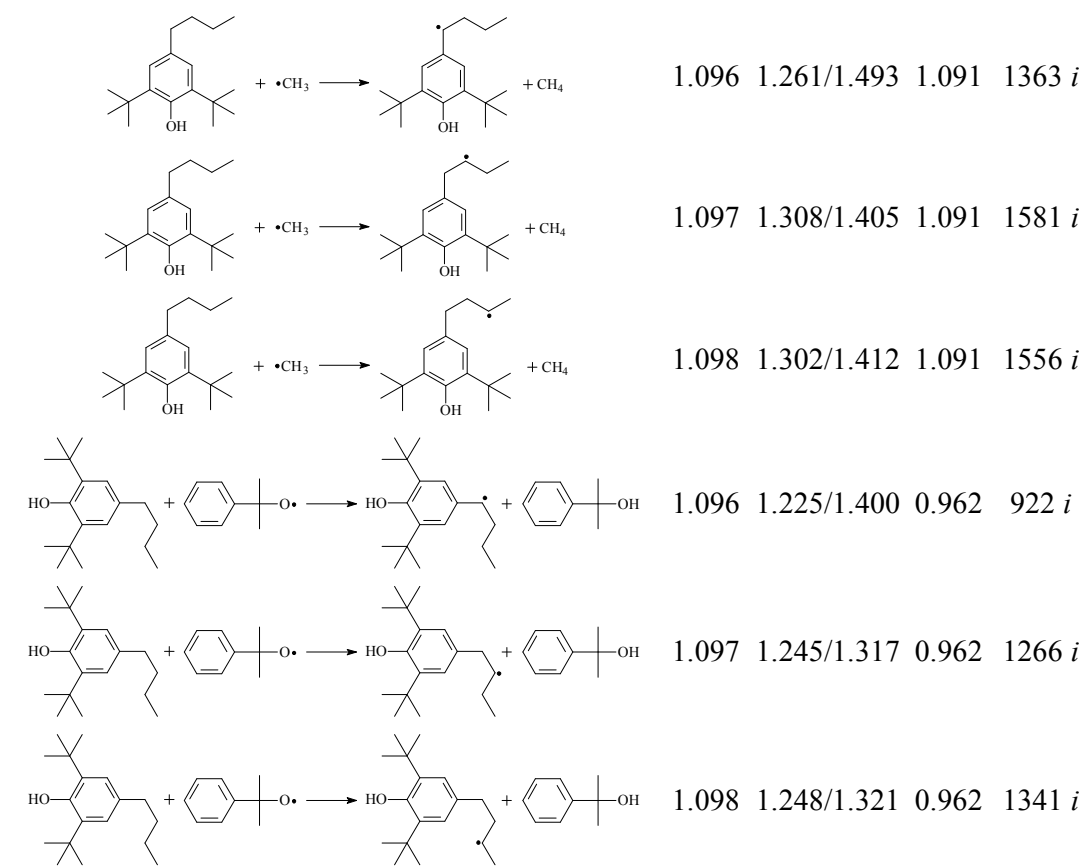
Table 2. The molecular formula, molecular name, and corresponding abbreviations of studied molecules.
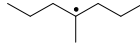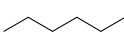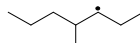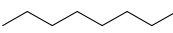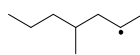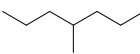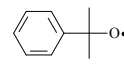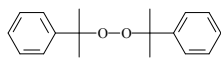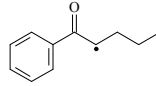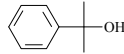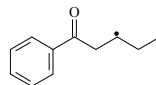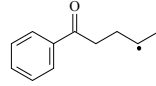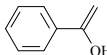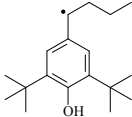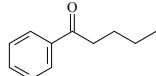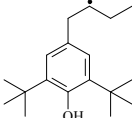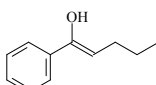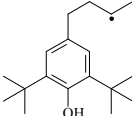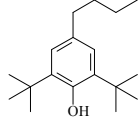
molecular formula	molecular name	ab.	molecular formula	ab.
	n-butane	4Pe		Pe84
	n-hexane	6Pe		Pe83
	n-octane	8Pe		Pe82
	4-methylheptane	Pe8		Cp
	dicumyl peroxide	DCp		Vp4
	2-phenyl-2-propanol	CpH		Vp3
	acetophenone	Ap		Vp2
	1-phenyl-1-ethenol	PAp		Bp4
	valerophenone	Vp		Bp3
	1-phenyl-1-pentenol	PVp		Bp2
	2,6-di-*t*-butyl-4-*n*-butylphenol	Bp	--	--

Table 3. The comparison of the adiabatic ionization potentials IP(a) and the electron affinities EA(a) (in unit of eV) for 6Pe, 8Pe, and Ap obtained from various theoretical optimizations and the experiment.

Method	Basis set	IP(a)			EA(a)
		6Pe	8Pe	Ap	Ap
HF[15]	6-31G*	9.18	9.06	7.77	-1.03
B3LYP[16-19]	6-31+G*	9.71	9.38	8.91	0.29
	6-311+G*	9.76	9.44	8.94	0.31
	6-311+G(d,p)	9.76	9.44	8.95	0.33
	6-311+G(3df,2p)	9.73	9.42	8.93	0.31
PBEPBE[20-21]	6-311+G(d,p)	9.43	9.05	8.65	0.41
MP2[22-24]	6-311+G(d,p)	--	--	9.61	-0.76
Exp.[25]		9.97	9.71±0.15	9.10±0.10	0.33

Table 4. The E_g, IPs, and EAs of studied molecules (in eV) calculated at the B3LYP/6-311+G(d,p) level as well as the corresponding experimental data in bracket.
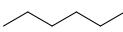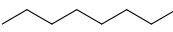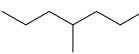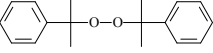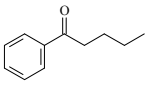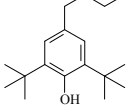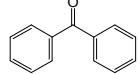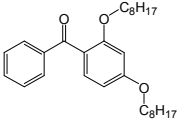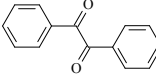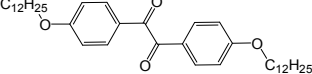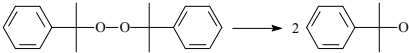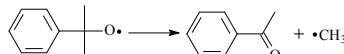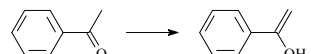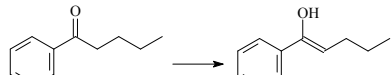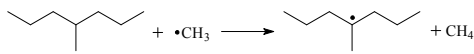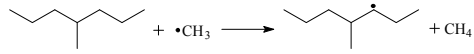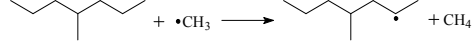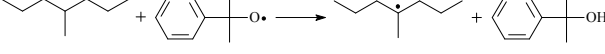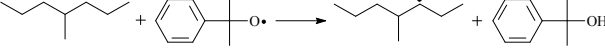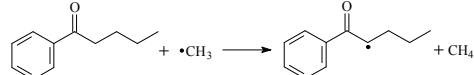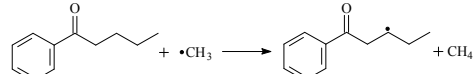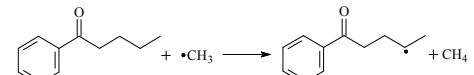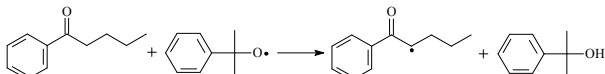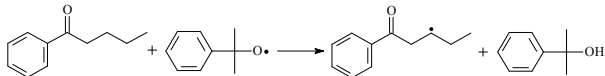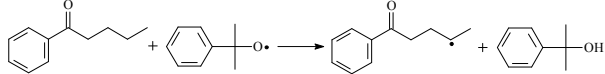
ab.	molecular formula	E_g	IP(a)	IP(v)	EA(a)	EA(v)
4Pe		9.09	10.15	8.84	-1.31	-1.31
6Pe		8.76	9.76 (9.97)	10.80	-1.20	-1.21
8Pe		8.52	9.44 (9.71 ± 0.15)	10.04	-1.12	-1.12
Pe8		8.38	9.41	10.03	-1.09	-1.10
DCP		5.75	7.79	8.11	1.76	-0.49
Ap		5.20	8.95 (9.10 ± 0.10)	9.19	0.33 (0.33)	0.09
Vp		5.19	8.79	8.94	0.33	0.15
Bp		5.62	7.20	7.49	-0.73	-0.74
Bz		4.90	8.64	8.67	0.73	0.50
Bzo		4.44	7.31	7.66	0.40	0.17
Ben		4.229	8.24	8.53	1.53	1.02
Bd		4.222	7.60	7.77	1.28	0.70

Table 5. The reaction enthalpies at 298 K (ΔH_{298}^0), the potential barrier heights TSs (ΔE^{TS}) with zero-point energy (ZPE) corrections for the studied reactions calculated on S_0 states at the B3LYP/6-311+G(d,p) levels (in eV), together with the breaking bond dissociation energies and BSSE energies of the corresponding transition states.

reaction equation	B3LYP/6-311+G(d,p)			
	ΔE^{TS}+ZPE	BSSE	ΔH_{298}^0	D_{298}^o
(reaction 1)	--	--	1.10	1.09
(reaction 2)	0.36	0.0206	-0.21	-0.27
(reaction 3)	2.70	0.0107	0.60	3.99
(reaction 4)	2.67	0.0100	0.57	3.72
(reaction 5)	0.43	0.0131	-0.47	3.91
(reaction 6)	0.51	0.0109	-0.352	4.041
(reaction 7)	0.47	0.0105	-0.38	4.01
(reaction 8)	0.249	0.0346	-0.40	3.91
(reaction 9)	0.33	0.0318	-0.28	4.041
(reaction 10)	0.24	0.0216	-0.31	4.01
(reaction 11)	0.36	0.0117	-0.69	3.72
(reaction 12)	0.491	0.0127	-0.340	4.053
(reaction 13)	0.47	0.0114	-0.354	4.038
(reaction 14)	0.230	0.0396	-0.62	3.72
(reaction 15)	0.37	0.0358	-0.264	4.053
(reaction 16)	0.226	0.0246	-0.28	4.038

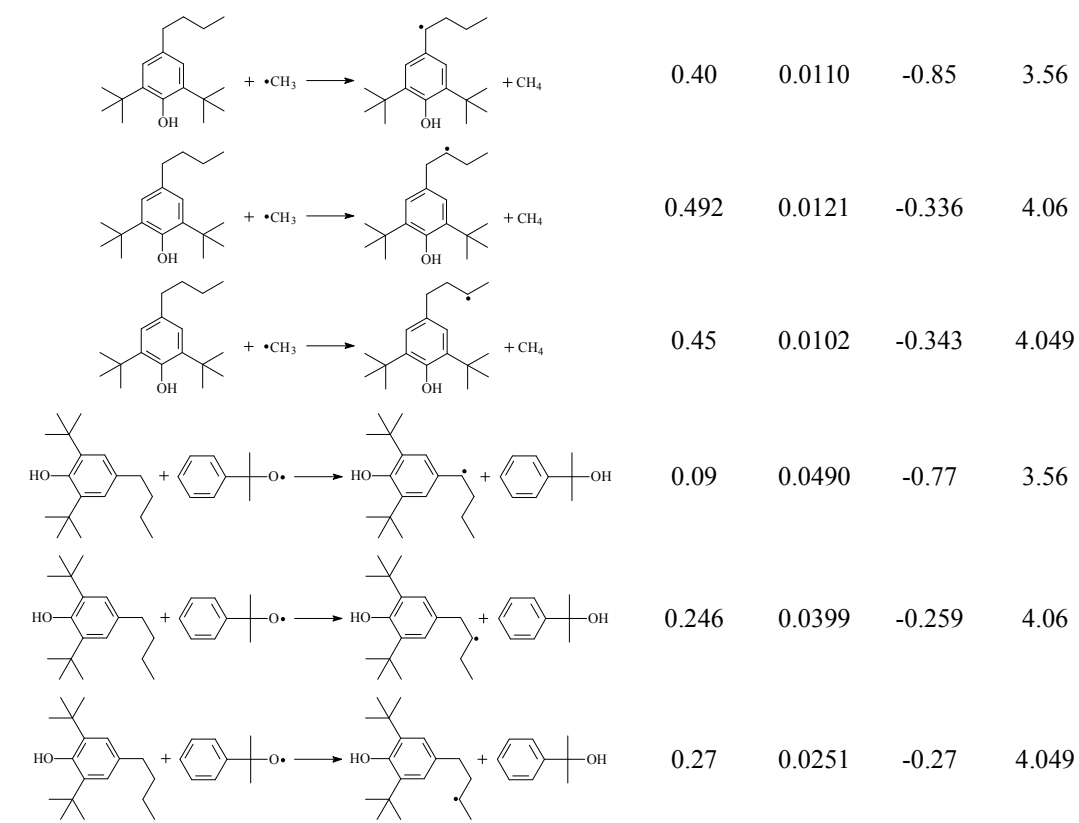|				
	0.40	0.0110	-0.85	3.56
	0.492	0.0121	-0.336	4.06
	0.45	0.0102	-0.343	4.049
	0.09	0.0490	-0.77	3.56
	0.246	0.0399	-0.259	4.06
	0.27	0.0251	-0.27	4.049

Figure Captions

Figure 1. Schematic description of geometric coordinate modifications and energy

changes.

Figure 2. Optimized geometric structures of the studied molecules at the

B3LYP/6-311+G(d,p) level.

Figure 1

Ap	TSAp	PAp	Vp	TSVp	PVp

Cp	TSCp	CpH	TSPe83	Pe84

Pe8	Dcp	TSPe82

Pe82	Pe83	TSPe84

TSVp2	TSVp3	TSVp4

Vp2	Vp3	Vp4

Ben	TSVp2Cp	TSVp3Cp

CH$_4$	Bp4	Bp2	Bp3
CH$_3$			

TSVp4Cp	TSPe82Cp	TSPe83Cp	TSPe84Cp
Bp	TSBp2	TSBp3	TSBp4

| TSBpCp2 | TSBpCp3 | TSBpCp4 |

Figure 2